

Multi-Wavelength High-Resolution Fourier Ptychographic Microscopy Using a Hemispherical LED Array

Mahdieh Gholami Mayani¹ ^a, Nazabat Hussain¹, Kim Robert Tekseth², Dag Werner Breiby^{1,2} and Muhammad Nadeem Akram¹

¹Department of Microsystems, University of South-Eastern Norway (USN), Norway

²Department of Physics, Norwegian University of Science and Technology (NTNU), Norway

Keywords: Fourier Ptychographic Microscopy, High Resolution, High Synthetic Numerical Aperture, Dome LED Array.

Abstract: Fourier Ptychographic microscopy has been proven to both increase the resolution of optical microscopes and retrieve the phase of objects using angular-varied illumination while maintaining a wide field-of-view. This work focuses on an improvement in the achieved half-pitch resolution, experimentally from 274 nm to 217 nm, by decreasing the operating wavelength from 630 nm to 470 nm. A high synthesized numerical aperture of 1.1 is obtained using 217 LEDs on a dome illuminator where the light is collected by a 10x/0.28NA objective lens. The experimental results closely match the theoretical prediction. As practical examples, two cartilage samples are analyzed and quantitatively imaged in this study.

1 INTRODUCTION

Providing wide field-of-view (FOV) and high resolution (HR) microscopy images is required for the statistical analysis of a huge number of biological cells simultaneously (Rimon and Schuldiner, 2011). Conventional microscopes suffer from a trade-off between spatial resolution and FOV. To tackle this problem, many efforts have been made such as mechanical scanning (Mico et al., 2006), and synthetic aperture scanning (Tippie et al., 2011). Fourier Ptychographic Microscopy (FPM) as a powerful imaging technique starts with capturing low resolution (LR) images where an array of light-emitting diode (LED) provides angular-varying partially coherent illumination (assumed as a coherent source) on the sample and a sequence of LR images are captured by a digital camera (Zheng et al., 2013), and (Zheng, 2016). The light coming from the sample is collected using a low numerical aperture (NA) objective lens which benefits from an inherent wide FOV. FPM then stitches the LR images together in Fourier space to achieve a high resolution (HR) image.

Optical aberrations, short depth of field, and no phase information from the sample of interest are shortcomings of current microscopes. FPM as a promising method can retrieve the unknown phase

of the imaged complex sample and digitally correct the existing aberration of the optical system. Two main parameters are involved to increase the microscopic resolved power and recovery efficiency: the operating wavelength λ and the NA. The FPM synthesized NA is described as $NA_{synth} = NA_{illum} + NA_{obj}$ where NA_{obj} is the fixed NA of the objective lens and NA_{illum} is the illumination NA. Using a planar LED board for illumination effectively limits NA_{illum} to less than about 0.5. Indeed, by increasing the incident angle, the signal-to-noise (SNR) ratio decreases and the dark field images contain more noise (Phillips et al., 2015). As such, a planar $x - y$ LED board with constant spacing between LEDs is not the optimum choice (Zheng et al., 2013). To break the mentioned constraints of commercially available planar LED boards, the dome geometry has been suggested which allows for sufficient SNR and higher NA with fewer LEDs, contributing to faster image acquisition and post-processing. Dome (Phillips et al., 2015), (Pan et al., 2018) and quasi-dome shaped LED array (Phillips et al., 2017), (Eckert et al., 2018), (Mayani et al., 2022b) configurations have been used. LEDs installed in a dome have much lower power falloff for off-axis LEDs as compared to planar board (Pan et al., 2018).

In the present study, a home-built hemispherical LED dome with 9 rings and 217 LEDs, yield-

^a  <https://orcid.org/0000-0002-4301-5734>

ing $NA_{illum} = 0.82$, has been made and integrated with FPM. We investigated three different illuminating wavelengths in the visible spectrum for FPM recovery of a USAF 1951 target, and then highly resolved images of two cartilage samples were obtained with the high NA_{synth} . This paper is organized as follows: Section 2 is devoted to reviewing the theoretical background of FPM. In section 3, the experimental results are presented and quantitatively compared. Finally, the conclusion and suggestions for future work are provided.

2 FPM THEORETICAL BACKGROUND

A schematic diagram of our FPM setup with a dome-shaped LED array is given in Fig.1 (Mayani et al., 2022b). The dome has been made of polymer using a 3D printing process and is controlled by a programmable Arduino board. The LEDs operate with central wavelength λ (different for red, green, and blue light) and they are implemented in specific positions, described by the polar angle θ and azimuthal angle ϕ of the spherical coordinate system. Each LED illumination is assumed to be quasi-monochromatic and spatially coherent. According to Fourier optics (Goodman, 2017), illuminating a sample from different angles leads to a shift in the object spatial frequency spectrum and thereby extends the transfer function beyond the cut-off frequency of the objective lens. The incident plane wave propagated from the n^{th} LED interacting with the thin specimen and having the transmission matrix $\bar{O}(x, y)$ can be modeled as $\bar{O}(x, y) \exp(jx \frac{2\pi}{\lambda} \sin(\theta_x), jy \frac{2\pi}{\lambda} \sin(\theta_y))$. Here, k_n is the oblique illumination from the corresponding LED and θ_x and θ_y are defined as incident angles with respect to the x and y axes, respectively (Mayani et al., 2022a). The optical system with a limited cut-off frequency can be modeled with a pupil function $P(k_x, k_y)$, in the spatial domain. The imaging can be described as

$$I = \left| \text{FFT}^{-1} \left[P(k_x, k_y) \text{FFT} \left(\bar{O}(x, y) \exp(jx \frac{2\pi}{\lambda} \sin(\theta_x), jy \frac{2\pi}{\lambda} \sin(\theta_y)) \right) \right] \right|^2 \quad (1)$$

$$= \left| \text{FFT}^{-1} \left[P(k_x, k_y) \bar{O}(k_x - \frac{2\pi}{\lambda} \sin(\theta_x), k_y - \frac{2\pi}{\lambda} \sin(\theta_y)) \right] \right|^2$$

wherein I represents the captured LR intensity image, and $\bar{O}(k_x, k_y)$ describes the object spatial spectrum. To satisfy the Nyquist criterion and avoid aliasing artifacts, the maximum frequency in the calculated spectrum is selected to be less than $1/(2\delta_x)$ (Konda, 2018) where δ_x is the spatial resolution. It is important to keep the pixel size of the LR matrix image below $\lambda/(2 NA_{obj})$ and similarly, for the HR matrix im-

age below $\lambda/(4 NA_{synth})$, thus avoiding possible out-of-band spurious signals. Accordingly, the maximum spatial frequency is given by $f_{max, synth} = NA_{synth}/\lambda$. Here, LEDs can be selected for their operating wavelength λ . To have an accurate FPM convergence, the object spectrum overlap between adjacent rings should be higher than 50% (Liu et al., 2016). LEDs must therefore be densely positioned in the central rings of the dome design, while they can be more sparsely spaced toward the outer rings. This arrangement leads to the necessity of fewer LED numbers as compared to the planar LED boards and in addition, a higher SNR is achieved for the dark-field images captured at larger illumination angles.

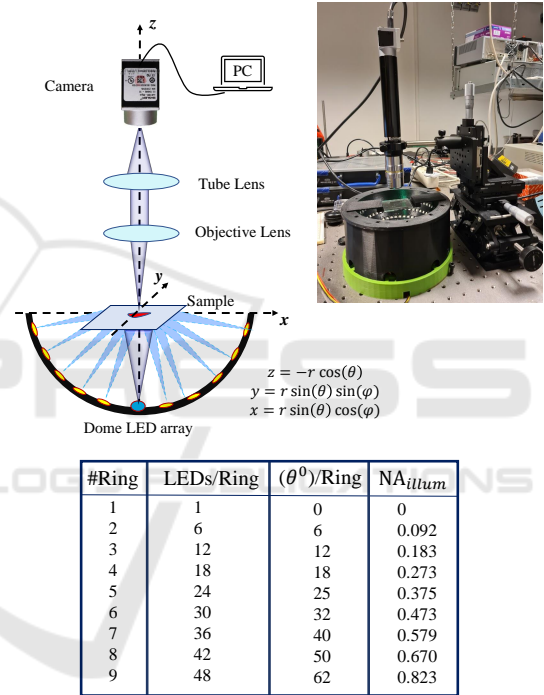


Figure 1: Schematic of the FPM setup. The LED sequences and NA_{synth} of each ring are listed in the provided table.

3 EXPERIMENTAL DEMONSTRATION: RESULTS AND COMPARISON

In this section, FPM is demonstrated with LR experimental images of a USAF 1951 test target (from *Ready Optics*), providing a standard resolution measurement. In this experiment, a $10\times/0.28NA$ objective lens collected the light coming from the sample and a digital camera (Basler acA5472-17um, 5496 \times 3672 pixels count) with $2.4 \mu\text{m}$ pixel size captured

the LR intensity images. To illuminate the sample, a home-built dome LED array was used wherein each LED (provided by NeoPixel) can work in the visible spectrum with the central wavelength λ ranging from 630 nm for the red light to 470 nm for blue light. According to the half-pitch resolution, defined as $\lambda/(2NA_{synth})$, the resolution is expected to increase when decreasing the illuminating wavelength. FPM setup reached a high $NA_{synth} = 1.1$ using the dome-shaped LED array. To reconstruct a HR image, a central patch of 512×512 pixels was selected on the LR images and the HR up-scaling ratio was set to 4. The theoretical half-pitch resolution is expected to increase from 283 nm to 211 nm when the illumination wavelength is changed from 630 nm to 470 nm. Fig. 2 shows a comparison between the recovered FPM HR complex-valued images. The cut-off frequency of the optical system is obtained slightly above the USAF target, group 10 element 6 with the standard resolution of 274 nm for the red color, and group 11 element 1 with the resolution of 244 nm for the green. For blue light, group 11 element 2 was successfully resolved, illustrating the resolution of 217 nm. The results are summarized in Table 1 and the recovered HR images are shown in Fig. 2. To practically demonstrate the performance of our FPM, two histological cartilage samples were studied, presented in Fig. 3. It is shown that high frequency details are clearly visible in the recovered images under the achieved NA_{synth} of 1.1. FPM in this study is based on transmission mode; however, the imaging technique can be extended to reflection mode.

Table 1: Comparison between theoretical and experimental resolution with three different operating wavelengths in the visible spectrum.

$\lambda_{illumination}$	Theoretical res	Experimental res
630 nm	283 nm	274 nm
530 nm	238 nm	244 nm
470 nm	211 nm	217 nm

4 CONCLUSIONS

In this paper, Fourier ptychographic microscopy imaging has been utilized to recover high-resolution images from a number of low-resolution images which correspond to angular-varied LED illumination. A home-built dome-shaped LED array was used to illuminate the sample, giving a synthetic numerical aperture (NA_{synth}) of 1.1. Three experiments have been carried out on the USAF test target and a comparison between results was demonstrated. There is an improvement in the resolution of the recovered

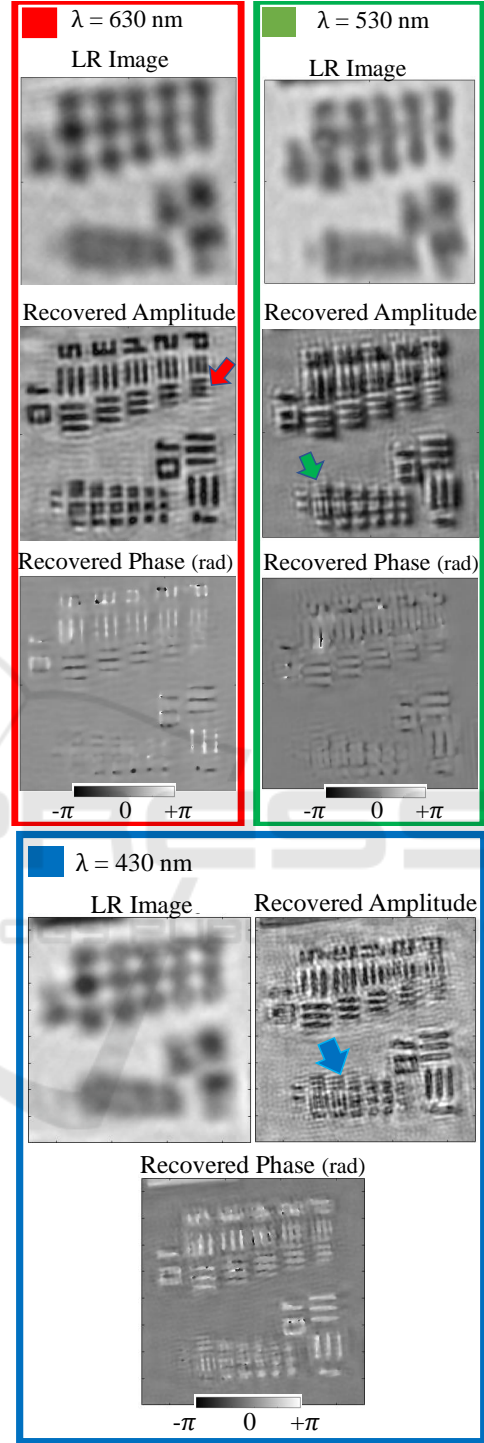


Figure 2: FPM recovery for the USAF amplitude test target: Recovered amplitude, and phase images corresponding to the red, green, and blue light illuminations. The resolved USAF elements are indicated by colored arrows.

images from 274 nm to 217 nm when the illuminating light is changed from wavelength 630 nm to 470

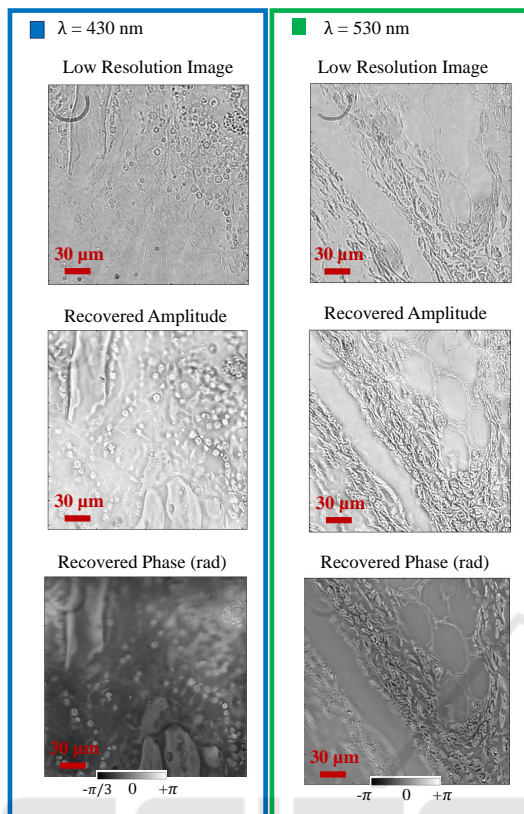


Figure 3: FPM amplitude and phase images of the cartilage samples obtained with the green and blue LEDs.

nm. There is a good agreement between the measurement and predicted theoretical values. Furthermore, two histological cartilage samples were examined as a practical example, showing a very fine details under the achieved high NA_{synth} by dome LED illuminator.

ACKNOWLEDGEMENTS

This work was supported by the Research Council of Norway through NANO2021 (project number 272248), and FRIPRO (project number 275182).

REFERENCES

- Eckert, R., Phillips, Z. F., and Waller, L. (2018). Efficient illumination angle self-calibration in fourier ptychography. *Appl. Opt.*, 57(19):5434–5442.
- Goodman, J. W. (2017). *Introduction to Fourier optics*. W.H. Freeman Macmillan Learning, New York, fourth edition. edition.
- Konda, P. C. (2018). *Multi-Aperture Fourier Ptychographic Microscopy: development of a high-speed gigapixel coherent computational microscope*. PhD dissertation, University of Glasgow.
- Liu, Q., Kuang, C., Fang, Y., Xiu, P., Li, Y., Wen, R., and Liu, X. (2016). Effect of spatial spectrum overlap on fourier ptychographic microscopy. *Journal of Innovative Optical Health Sciences*, 10.
- Mayani, M. G., Breiby, D. W., and Akram, M. N. (2022a). Polarization-sensitive Fourier ptychography microscopy using dome-shaped LED illuminator. In Georges, M. P., Popescu, G., and Verrier, N., editors, *Unconventional Optical Imaging III*, volume 12136, pages 31 – 34. International Society for Optics and Photonics, SPIE.
- Mayani, M. G., Hussain, N., Breiby, D. W., and Akram, M. N. (Aug 2022b). Improved resolution fourier ptychography scheme using oil-filled dome-shaped LED array. *Electronics Letters*, n/a(n/a).
- Mico, V., Zalevsky, Z., García-Martínez, P., and García, J. (2006). Synthetic aperture superresolution with multiple off-axis holograms. *Journal of the Optical Society of America. A, Optics, image science, and vision*, 23:3162.
- Pan, A., Zhang, Y., Wen, K., Zhou, M., Min, J., Lei, M., and Yao, B. (2018). Subwavelength resolution fourier ptychography with hemispherical digital condensers. *Opt. Express*, 26(18):23119–23131.
- Phillips, Z. F., D’Ambrosio, M. V., Tian, L., Rulison, J. J., Patel, H. S., Sadras, N., Gande, A. V., Switz, N. A., Fletcher, D. A., and Waller, L. (2015). Multi-contrast imaging and digital refocusing on a mobile microscope with a domed led array. *PLOS ONE*, 10:e0124938.
- Phillips, Z. F., Eckert, R., and Waller, L. (2017). Quasi-Dome: A Self-Calibrated High-NA LED Illuminator for Fourier Ptychography. *Imaging and Applied Optics 2017*, page IW4E.5.
- Rimon, N. and Schuldiner, M. (2011). Getting the whole picture: combining throughput with content in microscopy. *Journal of Cell Science*, 124(22):3743–3751.
- Tippie, A. E., Kumar, A., and Fienup, J. R. (2011). High-resolution synthetic-aperture digital holography with digital phase and pupil correction. *Opt. Express*, 19(13):12027–12038.
- Zheng, G. (2016). *Fourier Ptychographic Imaging*. 2053–2571. Morgan and Claypool Publishers.
- Zheng, G., Horstmeyer, R., and Yang, C. (2013). Wide-field, high-resolution Fourier ptychographic microscopy. *Nature Photonics 2013 7:9*, 7(9):739–745.